

CHARTS: Canadian-Chilean array for radio transient studies

Project presentation and system developments

Tomás Cassanelli

Universidad de Chile

July 25, 2025

FRB2025



tcassanelli@ing.uchile.cl



[charts-experiment](#)

Outline

- 1 FRB detection**
- 2 A new instrument: CHARTS**
- 3 Analog developments**
 - Antenna
 - Differential RF-chain
 - Multiplexing
- 4 Digital developments**
- 5 Summary**
- 6 References**



Presenting on behalf of students and co-I's
CHARTS collaboration

Millisecond transient radio sky

- Understand fast radio bursts (**FRBs**)
- All-sky FRB rate $\mathcal{R} \sim 10^3 \text{ d}^{-1}$
- Observational properties:
 - Duration of $t_w \sim \mu\text{s-ms}$
 - Broadband spectrum $\nu = \sim 0.2\text{--}6 \text{ GHz}$
 - Brightness temperature $T_b \sim 10^{40} \text{ K}$
 - Extreme energetics $E \sim 10^{35}\text{--}10^{45} \text{ erg}$
 - Some FRBs repeat $\sim 4\text{--}10 \%$

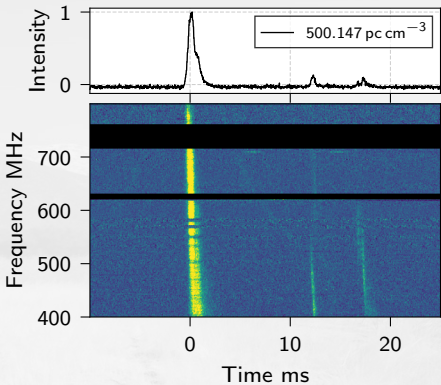


Figure: Fast radio burst (one-off) detected by the CHIME/FRB Collaboration, June 2021 ([Cassanelli et al. 2022](#)).

FRB detection: a \mathcal{R} and cost optimization

- FRB radio detection needs:
 - Large collector $A_e \rightarrow$ increased sensitivity $\Gamma \text{ K Jy}^{-1}$
 - Huge field-of-view $\Omega \rightarrow$ increased chance of detection
 - Angular resolution $\theta_{\text{res}} \rightarrow$ localization
- Solution: multi-beam radio interferometer with many beams!

$$\Gamma \propto A_e \propto 1/\theta_{\text{res}} \quad (1)$$

- FRB detection rate \mathcal{R} (CHIME/FRB Collaboration et al. 2021; Chawla et al. 2017)

$$\mathcal{R} \propto \Delta\nu^{0.75} n_a^{1.5} t_s^{-0.7} \quad (2)$$

- Bandwidth $\Delta\nu$: not heavily penalized
- Sampling time t_s is limited by the pulse width t_w



Figure: Canadian Hydrogen Intensity Mapping Experiment (CHIME) and its FRB backend (CHIME/FRB). Credits: Andre Renard.

FRB detection: a \mathcal{R} and cost optimization

- FRB radio detection needs:
 - Large collector $A_e \rightarrow$ increased sensitivity $\Gamma \text{ K Jy}^{-1}$
 - Huge field-of-view $\Omega \rightarrow$ increased chance of detection
 - Angular resolution $\theta_{\text{res}} \rightarrow$ localization
- Solution: multi-beam radio interferometer with many beams!

$$\Gamma \propto A_e \propto 1/\theta_{\text{res}} \quad (1)$$

- FRB detection rate \mathcal{R} ([CHIME/FRB Collaboration et al. 2021](#); [Chawla et al. 2017](#))

$$\mathcal{R} \propto \Delta\nu^{0.75} n_a^{1.5} t_s^{-0.7} \quad (2)$$

- Bandwidth $\Delta\nu$: not heavily penalized
- Sampling time t_s is limited by the pulse width t_w

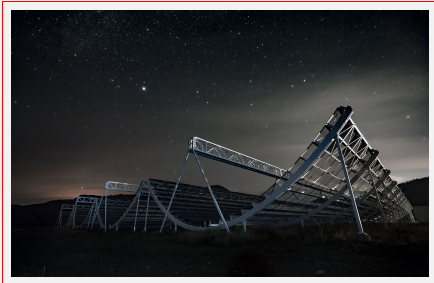


[Figure: Canadian Hydrogen Intensity Mapping Experiment \(CHIME\) and its FRB backend \(CHIME/FRB\). Credits: Andre Renard.](#)

Most FRBs have been found at high Dec

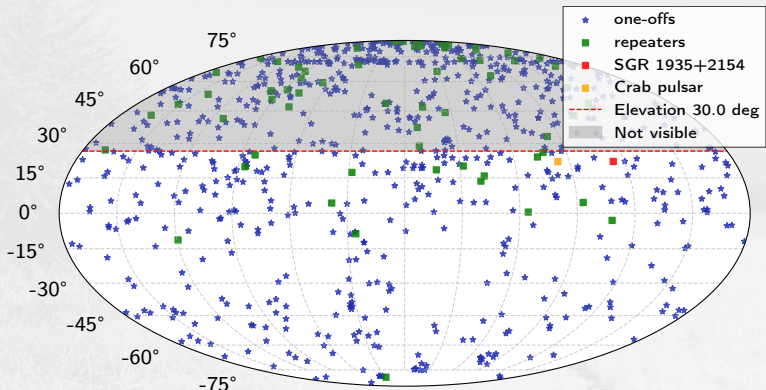


Figure: FRBs sky distribution in RA and Dec.

- Most FRBs have been detected above $\delta > 0^\circ$
- There are no long wavelength experiments in the Southern Hemisphere
- Less than $\sim 20\% \delta < 0^\circ$

A new radio interferometer: CHARTS

- Location: South America
- Exploit nearly empty sky at low latitudes
- A transient specific radio array
- Most experiments designed for multi-purpose besides transients
 - Limited FoV
 - Reduced monitoring capabilities
- The Galactic center has the potential of another **magnetar bright radio burst**
- Atacama region full with multiwavelength capabilities to follow-up

A new radio interferometer: CHARTS

- Location: South America
- Exploit nearly empty sky at low latitudes
- A transient specific radio array
- Most experiments designed for multi-purpose besides transients
 - Limited FoV
 - Reduced monitoring capabilities
- The Galactic center has the potential of another **magnetar bright radio burst**
- Atacama region full with multiwavelength capabilities to follow-up

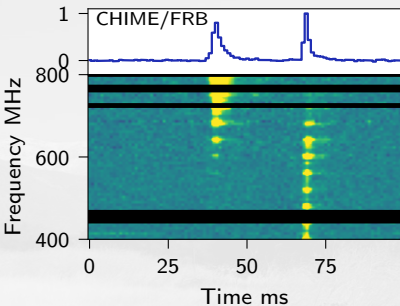


Figure: Magnetar SGR 1945+2154 in
[CHIME/FRB Collaboration et al. \(2020\)](#).

A new radio interferometer: CHARTS

- Location: South America
- Exploit nearly empty sky at low latitudes
- A transient specific radio array
- Most experiments designed for multi-purpose besides transients
 - Limited FoV
 - Reduced monitoring capabilities
- The Galactic center has the potential of another **magnetar bright radio burst**
- Atacama region full with multiwavelength capabilities to follow-up

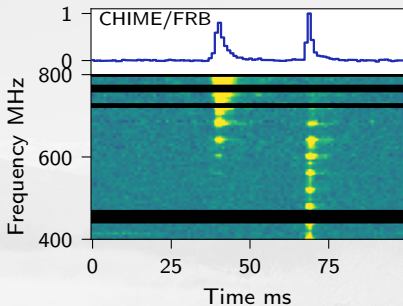


Figure: Magnetar SGR 1945+2154 in CHIME/FRB Collaboration et al. (2020).

CHARTS: Canadian-Chilean array for radio transient studies

CHARTS: Canadian-Chilean array for radio transient studies

- CHARTS a modest low-cost aperture array
- Multiplexed and differential RF architecture
- New generation digitizers (Xilinx RFSoC)
- Prioritized number of antennas: $\mathcal{R} \propto \Delta\nu^{0.75} n_a^{1.5}$

- $A_e \propto n_p n_a \lambda^2$; $n_a = 256$ single-pol
- HPBW $\approx 100^\circ$
- FoV: $\Omega = \Omega_a = 8 \times 10^3 \text{ deg}^2$
- 300–500 MHz passband

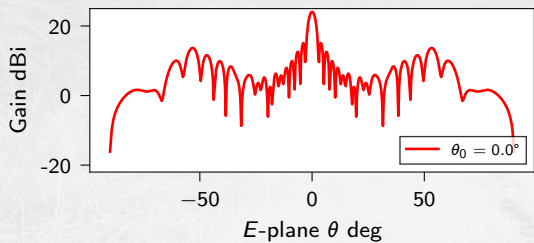
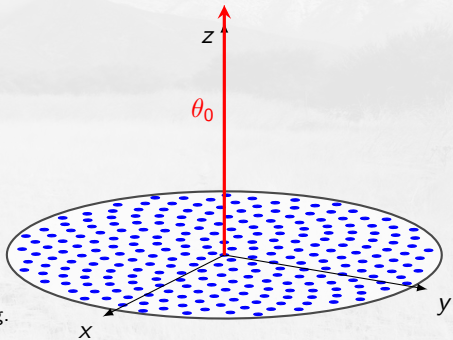


Figure: CHARTS configuration and beamforming.



CHARTS: Canadian-Chilean array for radio transient studies

- CHARTS a modest low-cost **aperture array**
- **Multiplexed and differential RF architecture**
- **New generation digitizers** (Xilinx RFSoC)
- **Prioritized number of antennas:** $\mathcal{R} \propto \Delta\nu^{0.75} n_a^{1.5}$
- $A_e \propto n_p n_a \lambda^2$; $n_a = 256$ single-pol
- HPBW $\approx 100^\circ$
- FoV: $\Omega = \Omega_a = 8 \times 10^3 \text{ deg}^2$
- 300–500 MHz passband

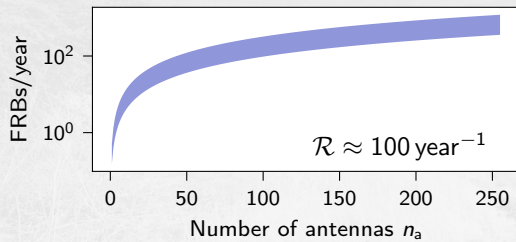
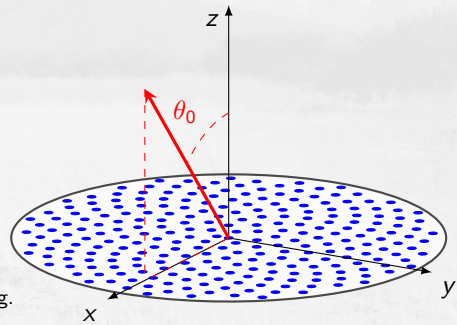


Figure: CHARTS configuration and beamforming.



CHARTS' scientific objectives

① Emission mechanisms

- Astrophysical process that produces FRBs

② FRB progenitors

- Identify sources and type of galaxy where they occur

③ Magnetar bursts and bright pulsar giant pulses

- Monitor local (Milky Way) phenomena that may be related to FRBs

④ New repeating FRBs

- Some FRBs repeat but less than 5% repeaters found in the South

- Optimized for bright FRBs
- FRBs slightly brighter near 400 MHz

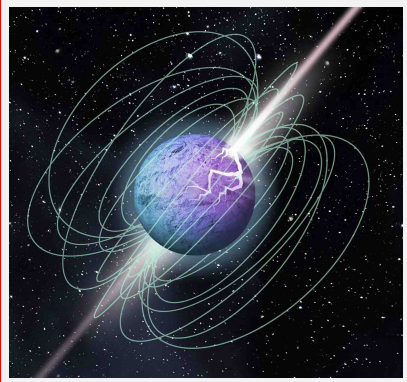
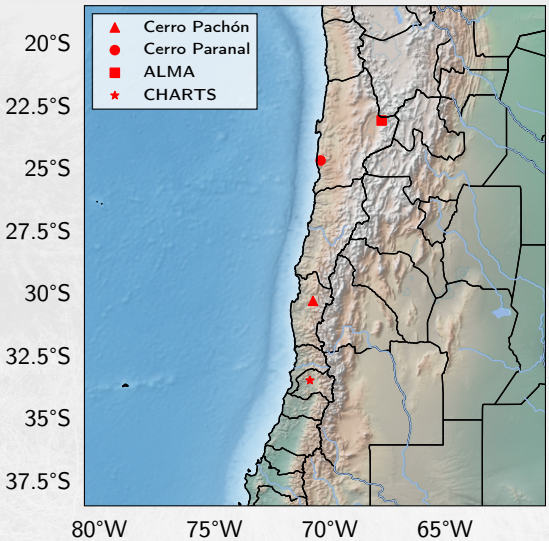
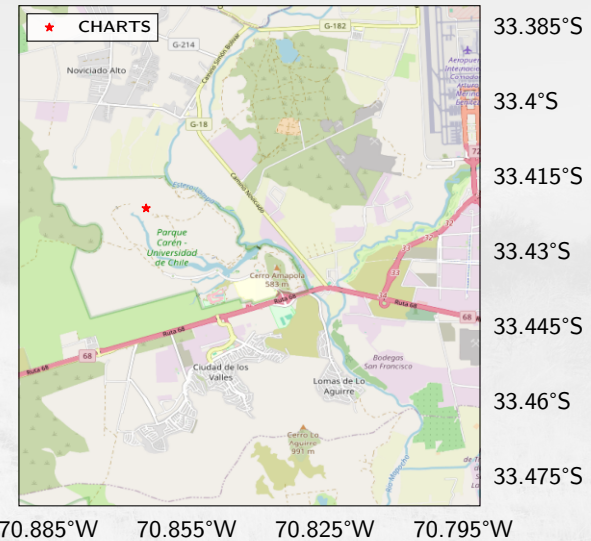


Figure: An artist's impression shows an outburst from a magnetar (McGill University Illustration).

CHARTS Earth location lat -33°



Cassanelli (UChile)



CHARTS-FRB2025

July 25, 2025

Site: Laguna Carén

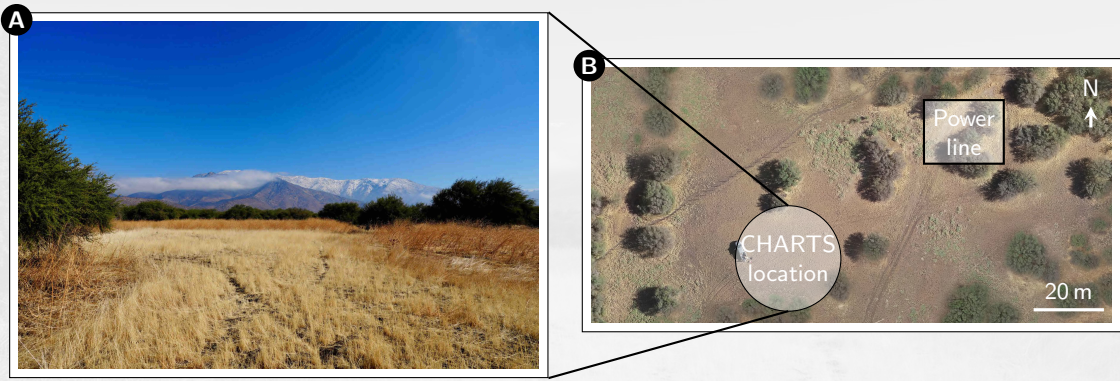


Figure: **A:** Laguna Carén site. **B:** View from the site. Array will cover $\sim 20\text{ m} \times 20\text{ m}$. Location is deep within the park with restricted access to the public.

Site: Laguna Carén

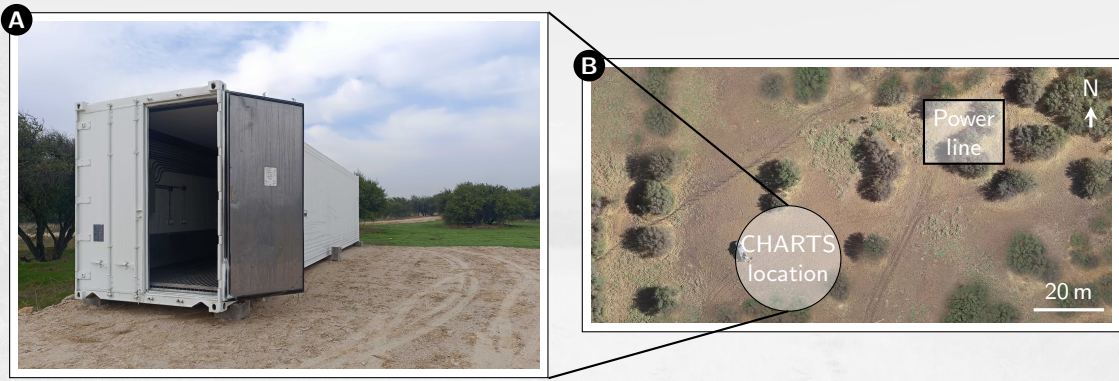


Figure: **A:** Laguna Carén site. **B:** View from the site. Array will cover $\sim 20\text{ m} \times 20\text{ m}$. Location is deep within the park with restricted access to the public.

CHARTS field-of-view Ω

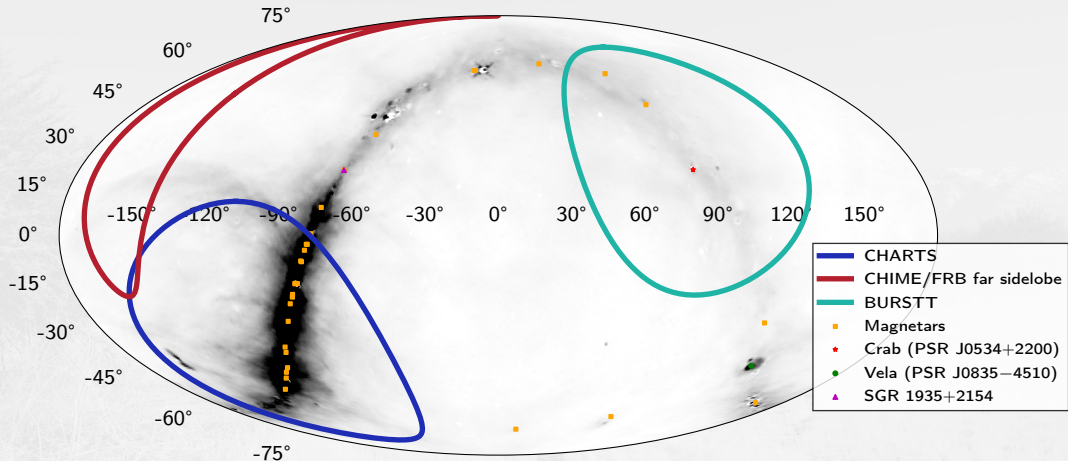


Figure: CHIME/FRB far sidelobe (Lin et al. 2024), BURSTT (Ling et al. 2023), and CHARTS FoV. Magnetars (Olausen & Kaspi 2014) and Galactic synchrotron background (300 MHz; BeyondPlanck Collaboration et al. 2023).

CHARTS field-of-view Ω

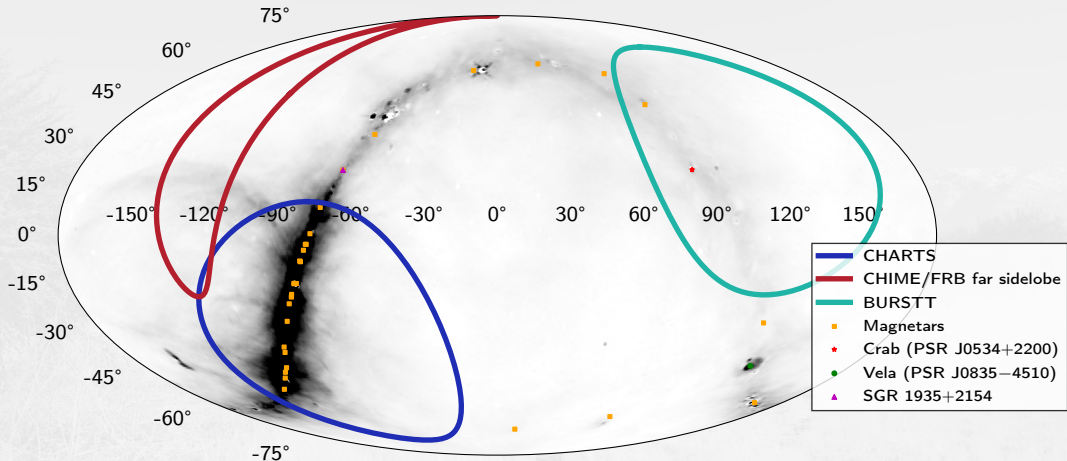


Figure: CHIME/FRB far sidelobe (Lin et al. 2024), BURSTT (Ling et al. 2023), and CHARTS FoV. Magnetars (Olausen & Kaspi 2014) and Galactic synchrotron background (300 MHz; BeyondPlanck Collaboration et al. 2023).

CHARTS field-of-view Ω

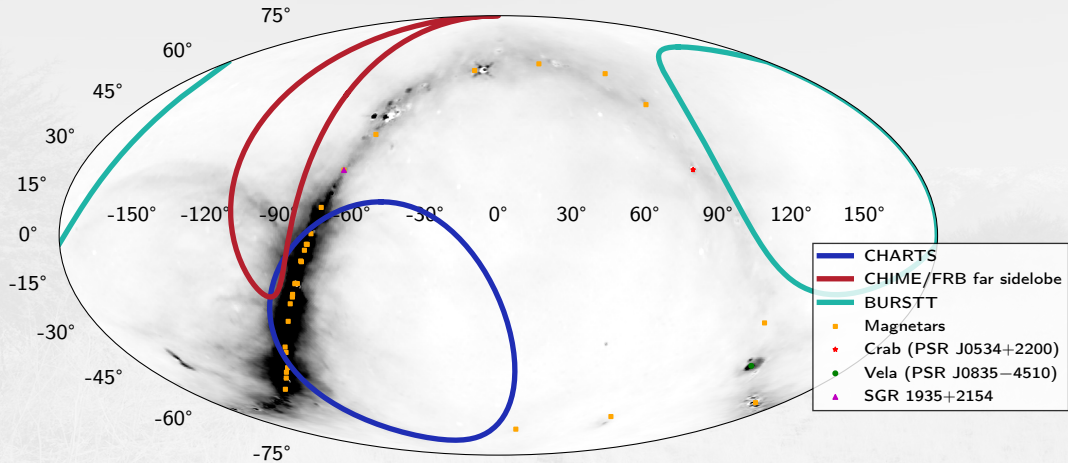


Figure: CHIME/FRB far sidelobe (Lin et al. 2024), BURSTT (Ling et al. 2023), and CHARTS FoV. Magnetars (Olausen & Kaspi 2014) and Galactic synchrotron background (300 MHz; BeyondPlanck Collaboration et al. 2023).

CHARTS field-of-view Ω

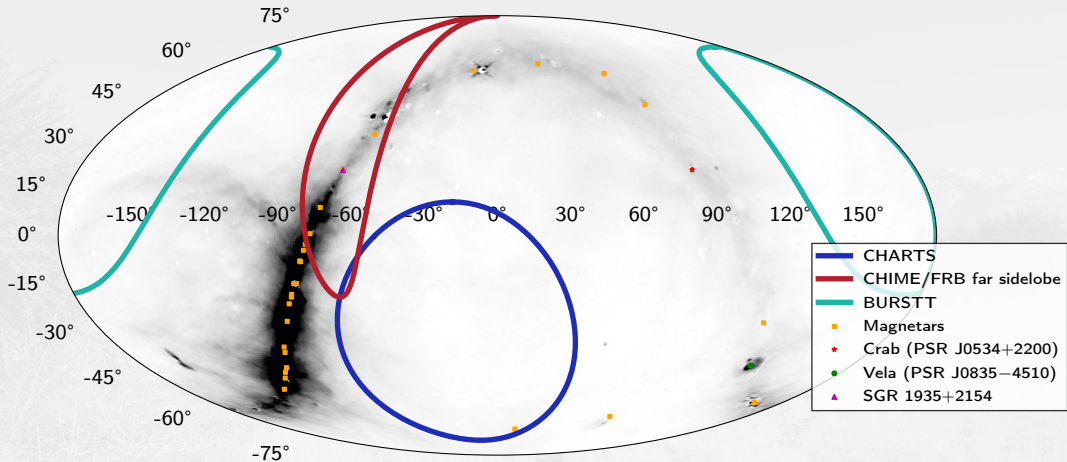


Figure: CHIME/FRB far sidelobe (Lin et al. 2024), BURSTT (Ling et al. 2023), and CHARTS FoV. Magnetars (Olausen & Kaspi 2014) and Galactic synchrotron background (300 MHz; BeyondPlanck Collaboration et al. 2023).

CHARTS field-of-view Ω

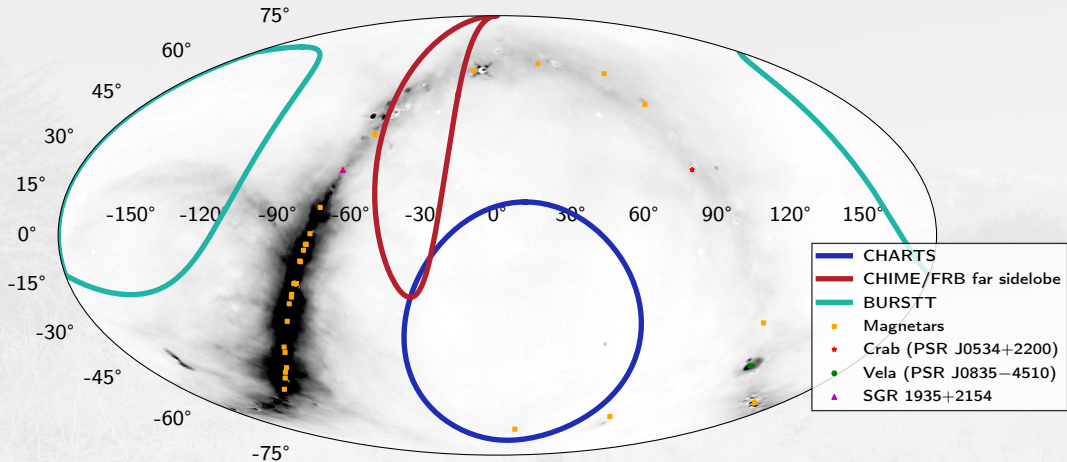


Figure: CHIME/FRB far sidelobe (Lin et al. 2024), BURSTT (Ling et al. 2023), and CHARTS FoV. Magnetars (Olausen & Kaspi 2014) and Galactic synchrotron background (300 MHz; BeyondPlanck Collaboration et al. 2023).

CHARTS field-of-view Ω

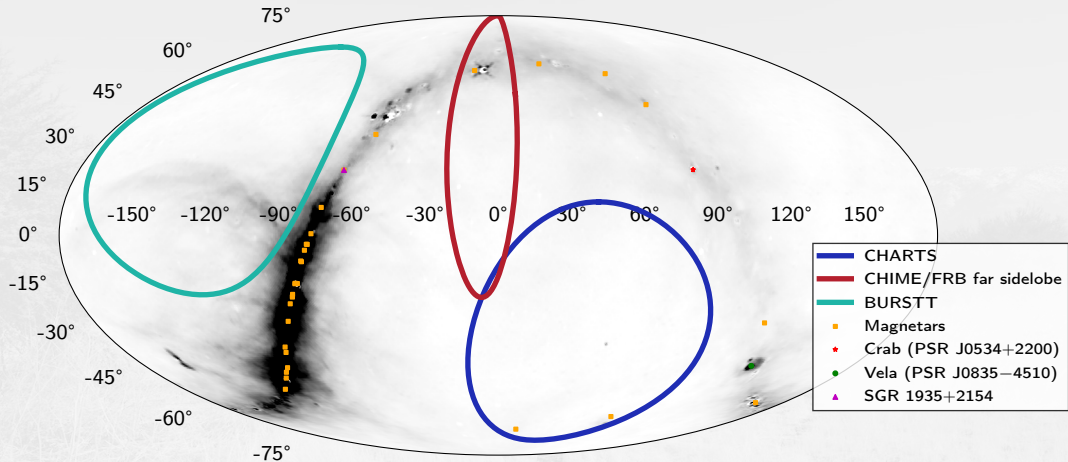


Figure: CHIME/FRB far sidelobe (Lin et al. 2024), BURSTT (Ling et al. 2023), and CHARTS FoV. Magnetars (Olausen & Kaspi 2014) and Galactic synchrotron background (300 MHz; BeyondPlanck Collaboration et al. 2023).

CHARTS field-of-view Ω

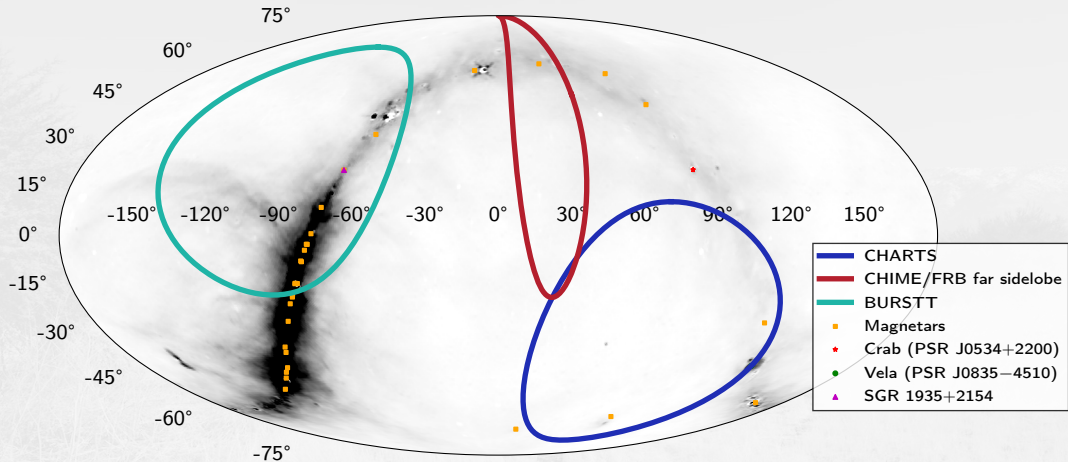


Figure: CHIME/FRB far sidelobe (Lin et al. 2024), BURSTT (Ling et al. 2023), and CHARTS FoV. Magnetars (Olausen & Kaspi 2014) and Galactic synchrotron background (300 MHz; BeyondPlanck Collaboration et al. 2023).

CHARTS field-of-view Ω

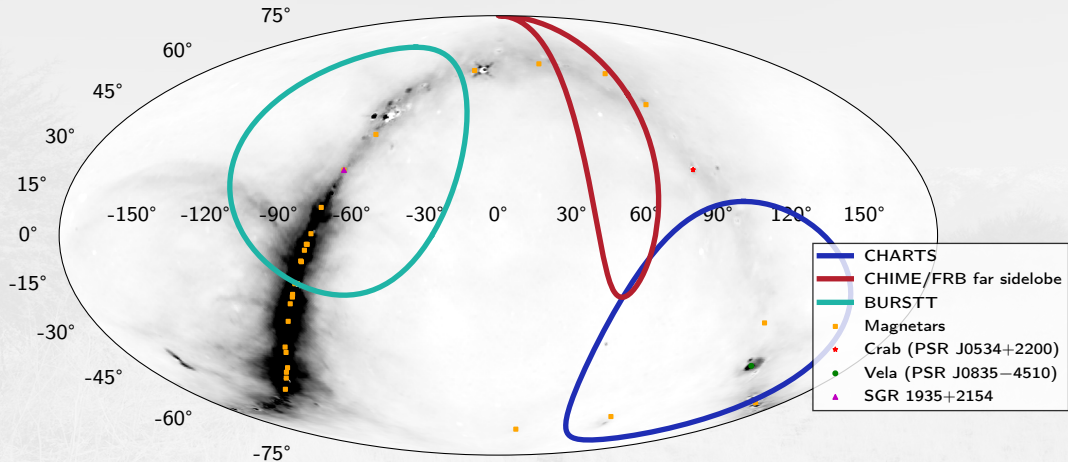


Figure: CHIME/FRB far sidelobe (Lin et al. 2024), BURSTT (Ling et al. 2023), and CHARTS FoV. Magnetars (Olausen & Kaspi 2014) and Galactic synchrotron background (300 MHz; BeyondPlanck Collaboration et al. 2023).

CHARTS field-of-view Ω

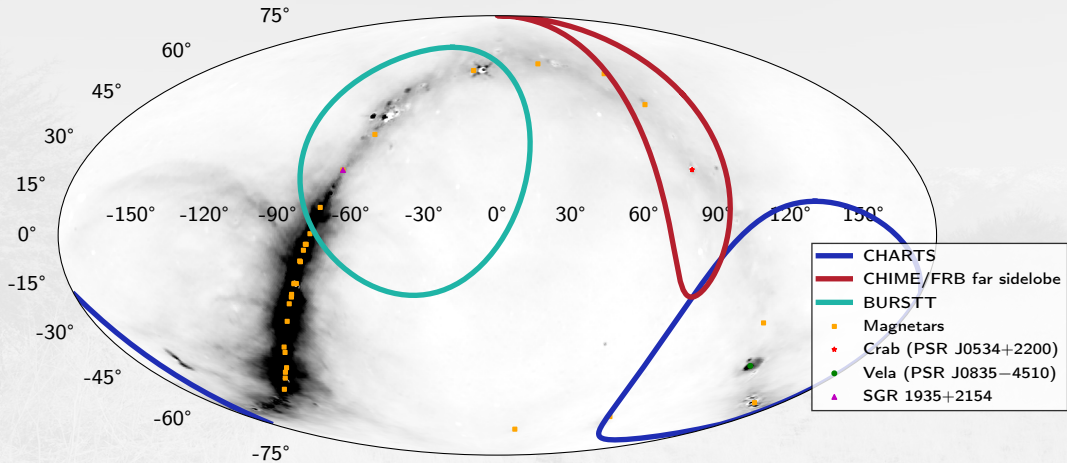


Figure: CHIME/FRB far sidelobe (Lin et al. 2024), BURSTT (Ling et al. 2023), and CHARTS FoV. Magnetars (Olausen & Kaspi 2014) and Galactic synchrotron background (300 MHz; BeyondPlanck Collaboration et al. 2023).

CHARTS field-of-view Ω

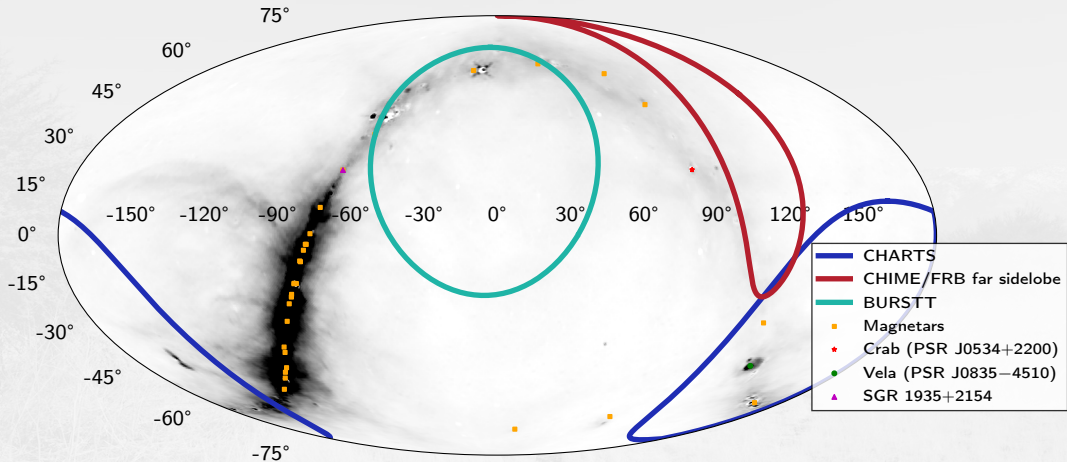


Figure: CHIME/FRB far sidelobe (Lin et al. 2024), BURSTT (Ling et al. 2023), and CHARTS FoV. Magnetars (Olausen & Kaspi 2014) and Galactic synchrotron background (300 MHz; BeyondPlanck Collaboration et al. 2023).

CHARTS field-of-view Ω

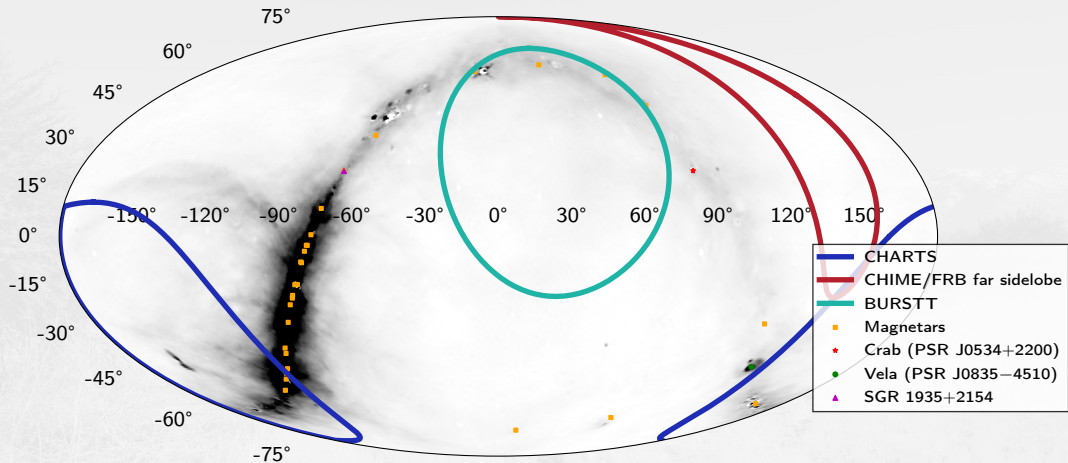


Figure: CHIME/FRB far sidelobe (Lin et al. 2024), BURSTT (Ling et al. 2023), and CHARTS FoV. Magnetars (Olausen & Kaspi 2014) and Galactic synchrotron background (300 MHz; BeyondPlanck Collaboration et al. 2023).

CHARTS field-of-view Ω

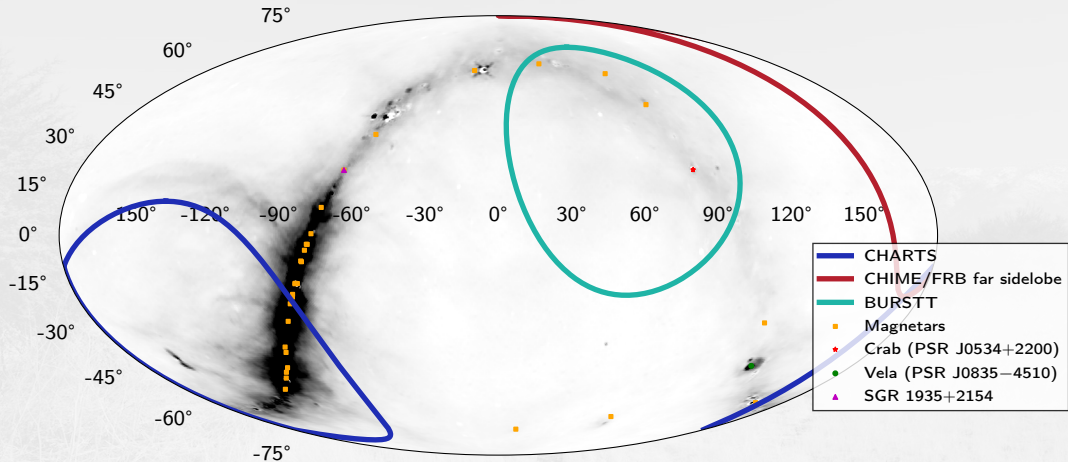


Figure: CHIME/FRB far sidelobe (Lin et al. 2024), BURSTT (Ling et al. 2023), and CHARTS FoV. Magnetars (Olausen & Kaspi 2014) and Galactic synchrotron background (300 MHz; BeyondPlanck Collaboration et al. 2023).

Antenna developments HPBW \approx 90 deg

- A planar printed antenna
- Differential $Z_a = 100\text{--}130 \Omega$
- Led by: Dr. Albert Wai Kit Lau
- HPBW \approx 90 deg
- $\sim 7 \text{ dBi}$
- Aperture array Ω is the antenna FoV Ω_a
- $T_{\text{sys}} < 50 \text{ K}$

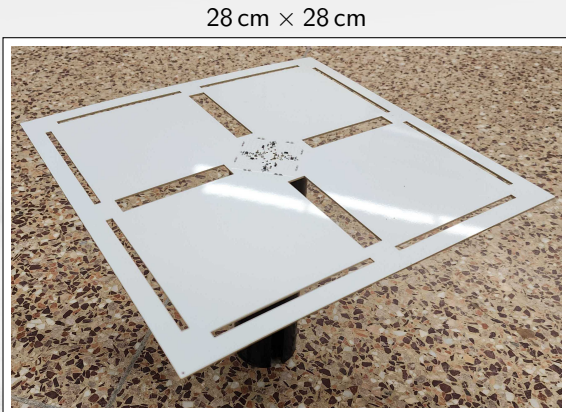


Figure: Differential antenna 300–500 MHz.

Antenna developments HPBW \approx 90 deg

- A planar printed antenna
- Differential $Z_a = 100\text{--}130 \Omega$
- Led by: **Dr. Albert Wai Kit Lau**
- HPBW \approx 90 deg
- $\sim 7 \text{ dBi}$
- Aperture array Ω is the antenna FoV Ω_a
- $T_{\text{sys}} < 50 \text{ K}$



Figure: Differential antenna 300–500 MHz.

Antenna developments HPBW \approx 90 deg

- A planar printed antenna
- Differential $Z_a = 100\text{--}130 \Omega$
- Led by: Dr. Albert Wai Kit Lau
- HPBW \approx 90 deg
- $\sim 7 \text{ dBi}$
- Aperture array Ω is the antenna FoV Ω_a
- $T_{\text{sys}} < 50 \text{ K}$

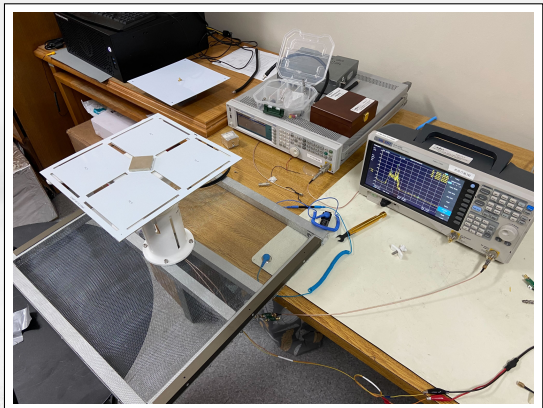
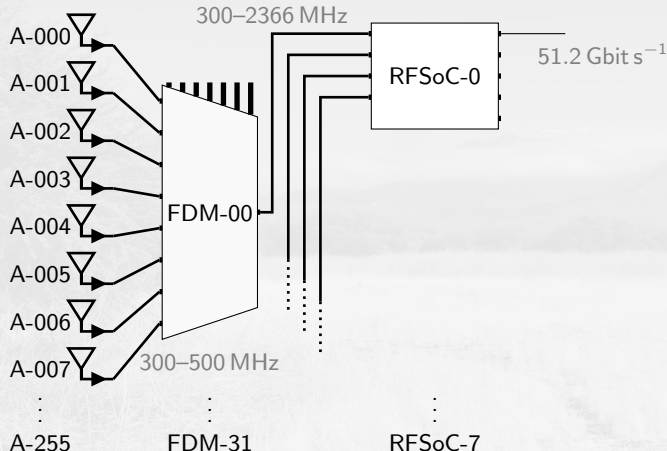


Figure: Differential antenna 300–500 MHz.

Radio frequency chain



- Passband 300–500 MHz
- $\Delta\nu = 200$ MHz
- Frequency division multiplexer (FDM)
- Xilinx RFSoC digitizer
- 32 antennas per digitizer
- 1 FDM every 8 antennas
- CHARTS analog components:
 - 256 antennas
 - 32 Multiplexers
 - 8 RFSoC
- Differential implementation: $Z \neq 50 \Omega$
- Effective bandwidth 2.45 GHz
- Entire system: 410 Gbit s⁻¹

Figure: Radio frequency chain for 256 antennas.

Radio frequency chain

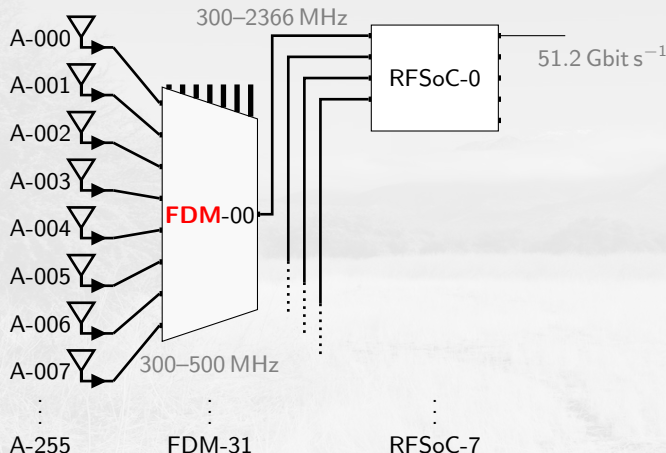


Figure: Radio frequency chain for 256 antennas.

- Passband 300–500 MHz
- $\Delta\nu = 200$ MHz
- **Frequency division mutiplexer (FDM)**
- Xilinx RFSoC digitizer
- 32 antennas per digitizer
- 1 FDM every 8 antennas
- CHARTS analog components:
 - 256 antennas
 - 32 Multiplexers
 - 8 RFSoC
- Differential implementation: $Z \neq 50 \Omega$
- Effective bandwidth 2.45 GHz
- Entire system: 410 Gbit s⁻¹

Radio frequency chain

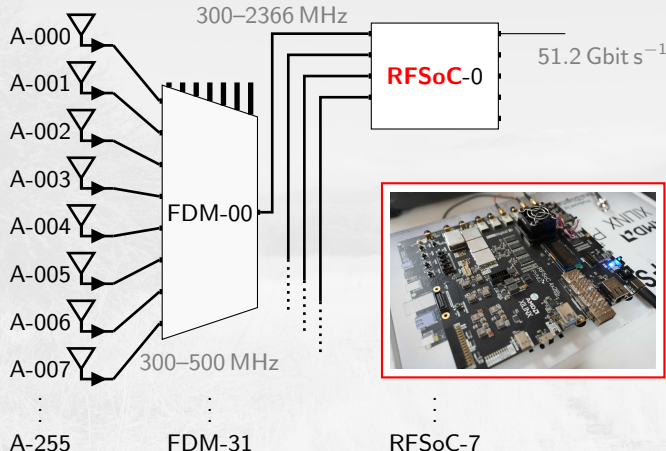
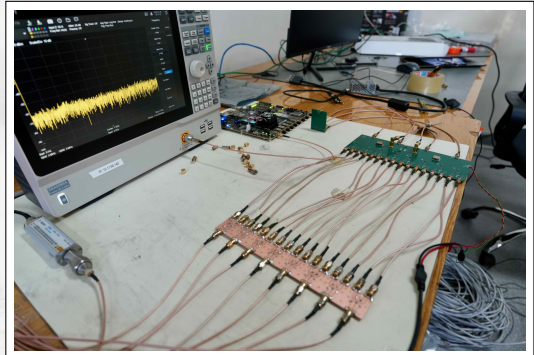
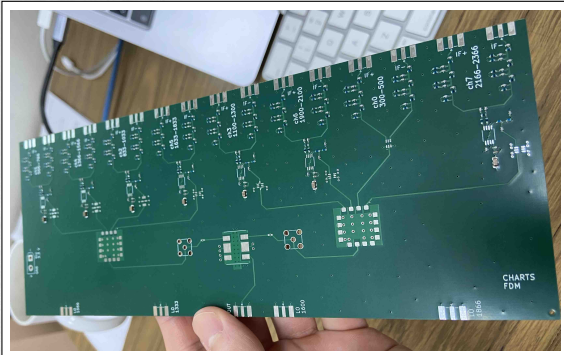


Figure: Radio frequency chain for 256 antennas.

- Passband 300–500 MHz
- $\Delta\nu = 200$ MHz
- Frequency division multiplexer (FDM)
- **Xilinx RFSoC digitizer**
- 32 antennas per digitizer
- 1 FDM every 8 antennas
- CHARTS analog components:
 - 256 antennas
 - 32 Multiplexers
 - 8 RFSoC
- Differential implementation: $Z \neq 50 \Omega$
- Effective bandwidth 2.45 GHz
- Entire system: 410 Gbit s⁻¹

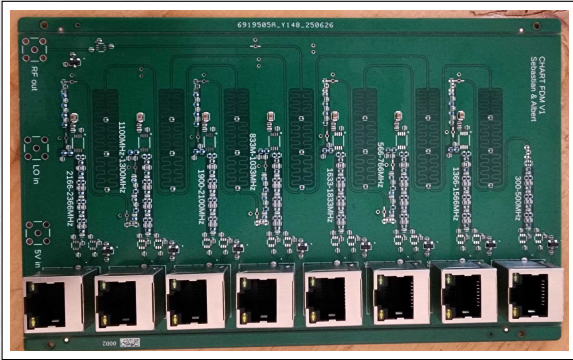
Frequency division multiplexer (FDM) development

- Lead by MSc. Sebastián Manosalva
- Full band: 300–2400 MHz
- Differential impedance
- Electrical length, coupling, isolation, impedance matching, bias-tee, baluns, not a simple project!



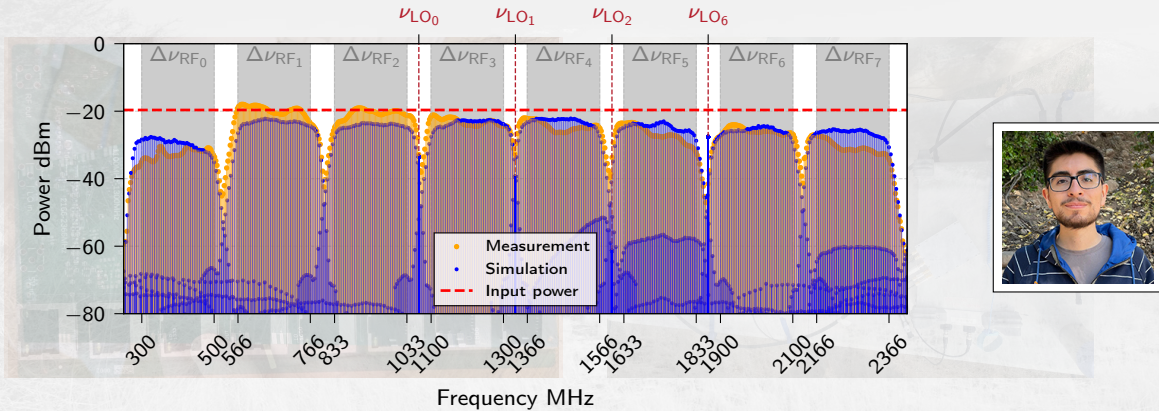
Frequency division multiplexer (FDM) development

- Lead by MSc. Sebastián Manosalva
- Full band: 300–2400 MHz
- Differential impedance
- Electrical length, coupling, isolation, impedance matching, bias-tee, baluns, not a simple project!



Frequency division multiplexer (FDM) development

- Lead by MSc. **Sebastián Manosalva**
- Full band: 300–2400 MHz
- Differential impedance
- Electrical length, coupling, isolation, impedance matching, bias-tee, baluns, not a simple project!



F-engine: RFSoC demux implementation

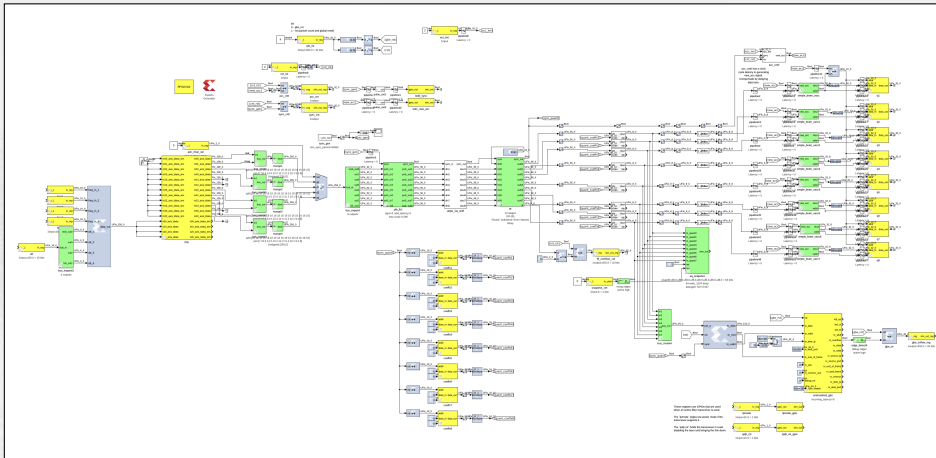


Figure: CASPER-based (Hickish et al. 2016) spectrometer in RFSoC 4x2. Led by Bruno Pollaro.

F-engine: RFSoC demux implementation

4 + 4 bit
Fourier Transform
demux
LO tones
Linked to 100 GbitE

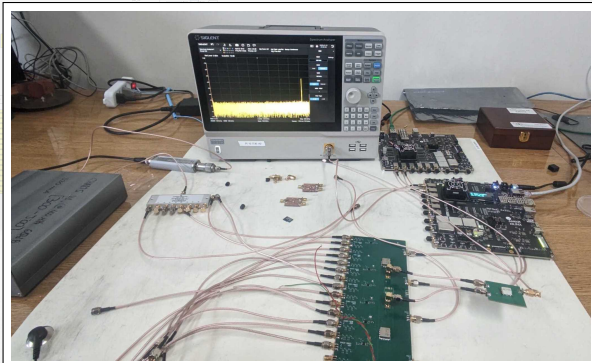
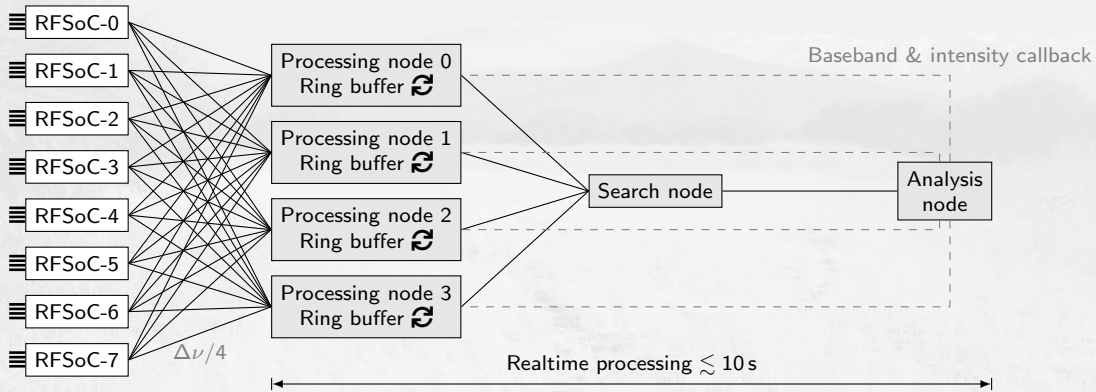
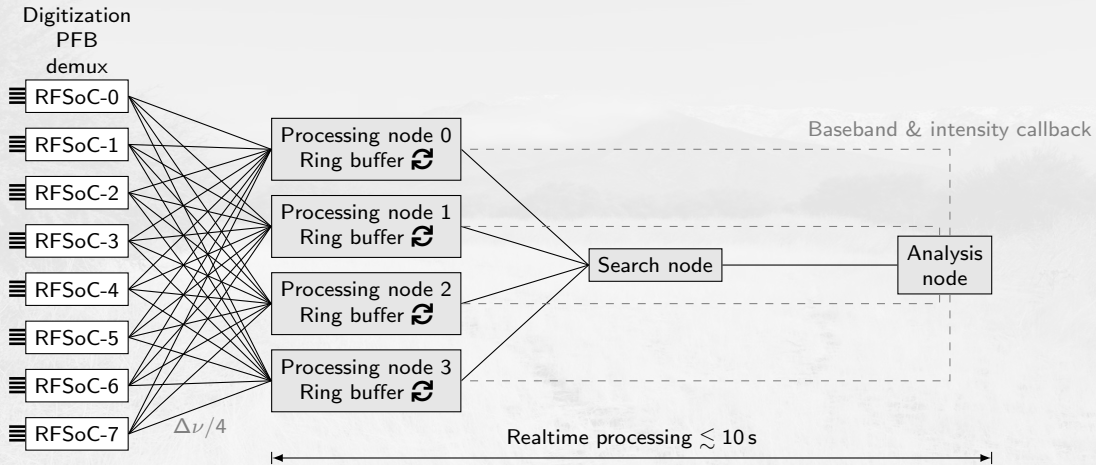


Figure: CASPER-based (Hickish et al. 2016) spectrometer in RFSoC 4x2. Led by **Bruno Pollaro**.

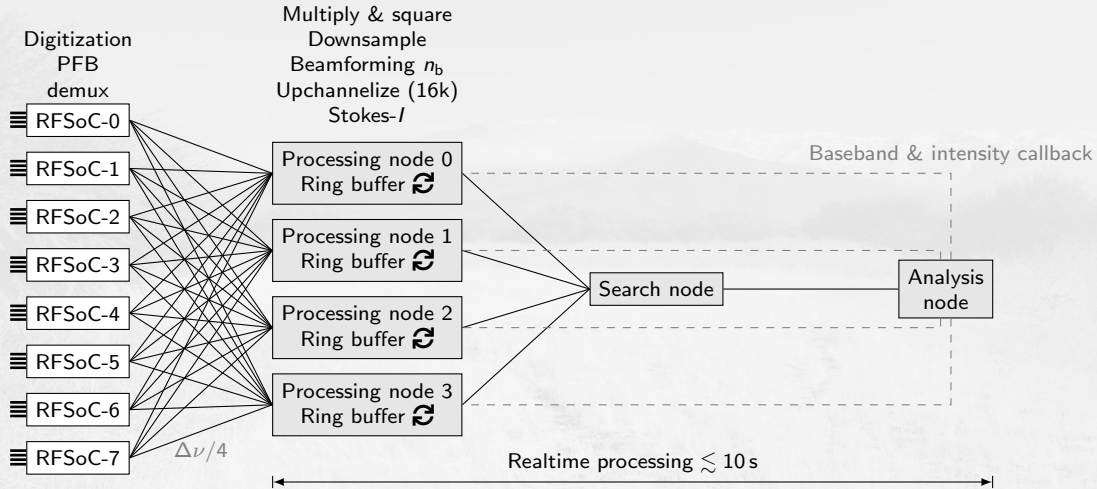
FX-engine architecture



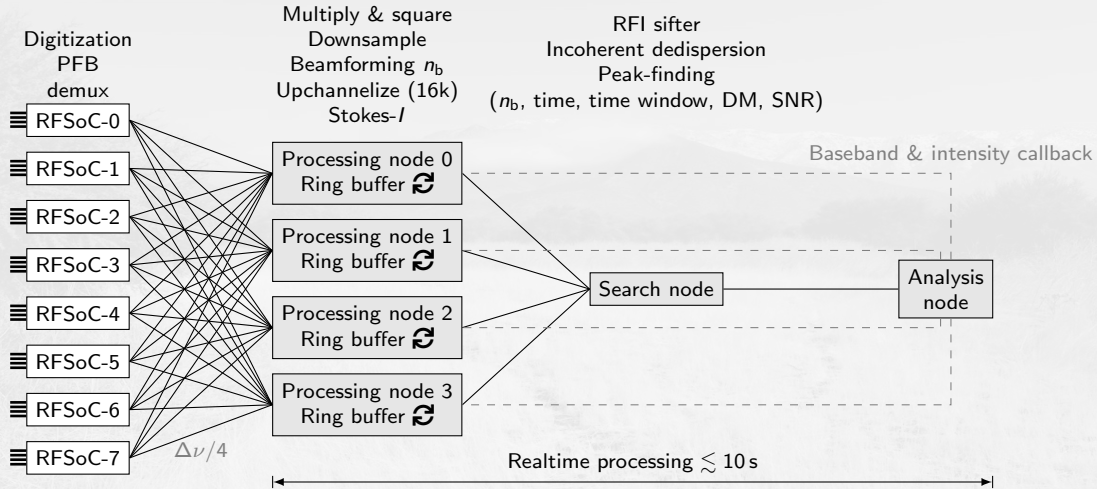
FX-engine architecture



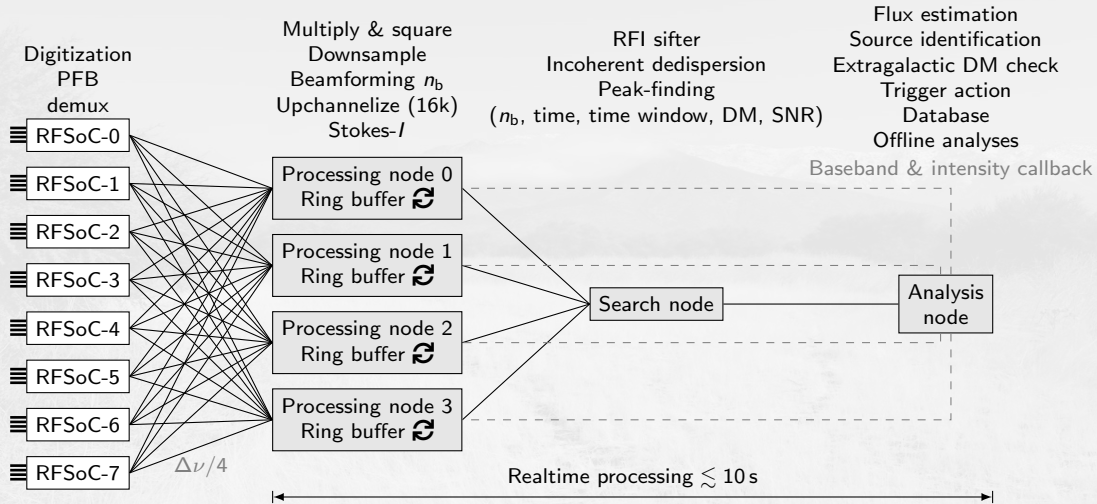
FX-engine architecture



FX-engine architecture



FX-engine architecture



FX-engine architecture

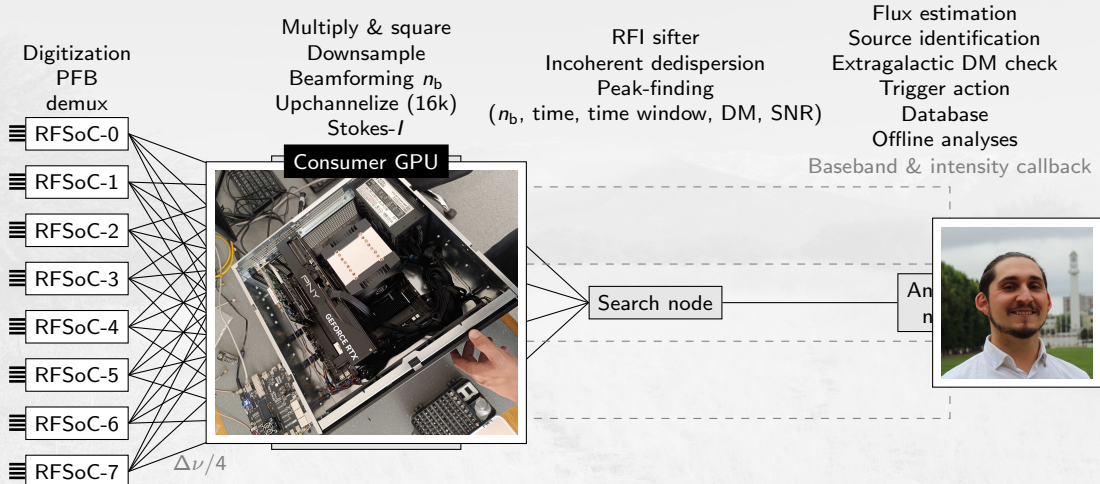


Figure: X-engine developed by MSc. **Gonzalo Burgos**.

CHARTS-8 prototype and preliminar performance

CHARTS-8

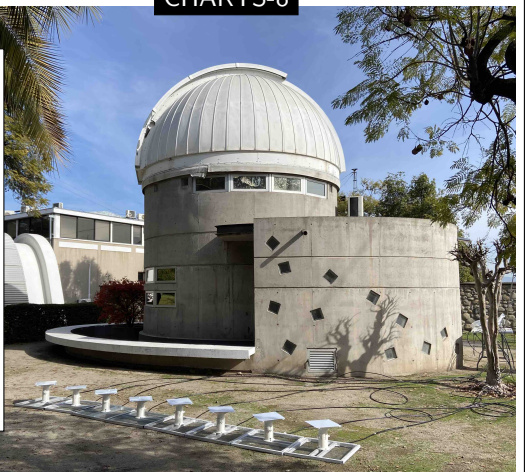


Figure: CHARTS-8 prototype at
Universidad de Chile.

CHARTS-8 prototype and preliminar performance

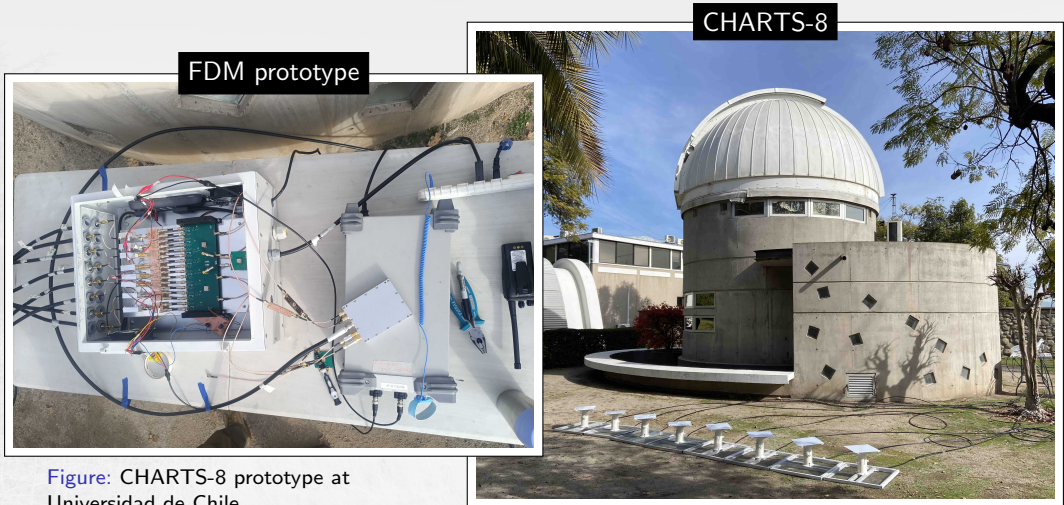


Figure: CHARTS-8 prototype at Universidad de Chile.

CHARTS-8 prototype and preliminar performance

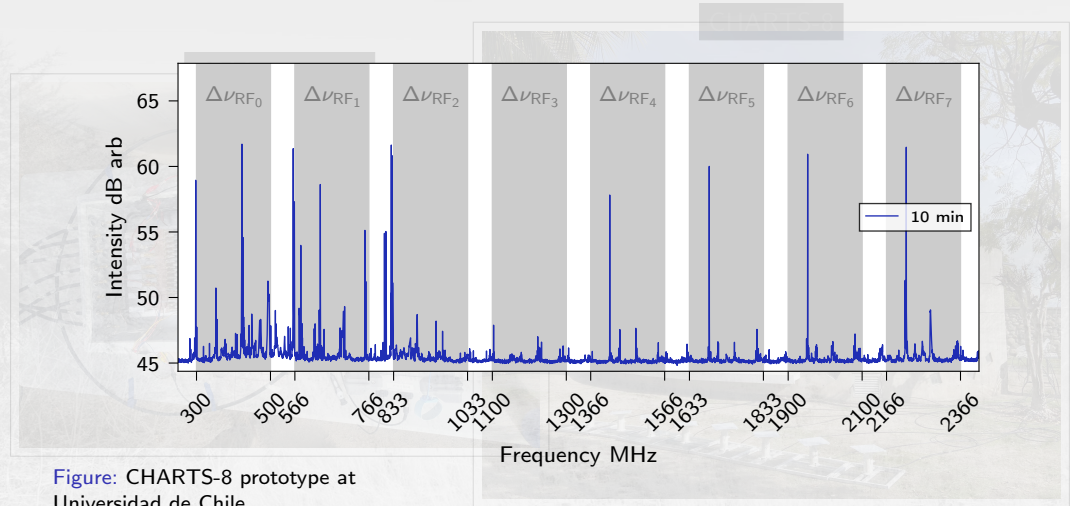


Figure: CHARTS-8 prototype at Universidad de Chile.

Summary and takeaways

Table: CHARTS parameter summary.

Parameter	Value
Antenna beam (HPBW)	90 deg
Antenna polarization number n_p	1
Bandwidth $\Delta\nu$	200 MHz
Channel bandwidth	300 kHz
Field-of-view (FoV)	$\sim 8 \times 10^3$ deg 2
Frequency channels	~ 600
Number of antennas n_a	256
Number of beams n_b	10^3
Passband	300–500 MHz
Search sample time (t_s)	1 ms
Sample time (t_s)	3 μ s
System temperature T_{sys}	50 K

- CHARTS: a modest instrument a great impact
- To be built entirely at university level
- Optimized for \mathcal{R} and cost
- We prioritize n_a rather than $\Delta\nu$
- Cost impact:
 - Custom optimized antenna
 - FDM → less digitizers
 - Differential RF
 - Consumer GPUs
- CHARTS-32 January 2026

Summary and takeaways

Table: CHARTS parameter summary.

Parameter	Value
Antenna beam (HPBW)	90 deg
Antenna polarization number n_p	1
Bandwidth $\Delta\nu$	200 MHz
Channel bandwidth	300 kHz
Field-of-view (FoV)	$\sim 8 \times 10^3$ deg 2
Frequency channels	~ 600
Number of antennas n_a	256
Number of beams n_b	10^3
Passband	300–500 MHz
Search sample time (t_s)	1 ms
Sample time (t_s)	3 μ s
System temperature T_{sys}	50 K

- CHARTS: a modest instrument a great impact
- To be built entirely at university level
- Optimized for \mathcal{R} and cost
- We prioritize n_a rather than $\Delta\nu$
- Cost impact:
 - Custom/optimized antenna
 - FDM \rightarrow less digitizers
 - Differential RF
 - Consumer GPUs
- CHARTS-32 January 2026

Summary and takeaways

Table: CHARTS parameter summary.

Parameter	Value
Antenna beam (HPBW)	90 deg
Antenna polarization number n_p	1
Bandwidth $\Delta\nu$	200 MHz
Channel bandwidth	300 kHz
Field-of-view (FoV)	$\sim 8 \times 10^3$ deg 2
Frequency channels	~ 600
Number of antennas n_a	256
Number of beams n_b	10^3
Passband	300–500 MHz
Search sample time (t_s)	1 ms
Sample time (t_s)	3 μ s
System temperature T_{sys}	50 K

- CHARTS: a modest instrument a great impact
- To be built entirely at university level
- Optimized for \mathcal{R} and cost
- We prioritize n_a rather than $\Delta\nu$
- Cost impact:
 - Custom/optimized antenna
 - FDM \rightarrow less digitizers
 - Differential RF
 - Consumer GPUs
- **CHARTS-32 January 2026**

CHARTS and beyond

- Pathfinder CHARTS-8
- **CHARTS** will start operating mid-2026 24/7 operations
- CHARTS will find $\mathcal{R}_{\text{CHARTS}} \approx 100 \text{ year}^{-1}$
- CHARTS will localize bright and nearby low-DM FRBs
- Collaboration at multiwavelength followups
- **CHARTS white paper in prep.!**

¡Gracias! Thanks!

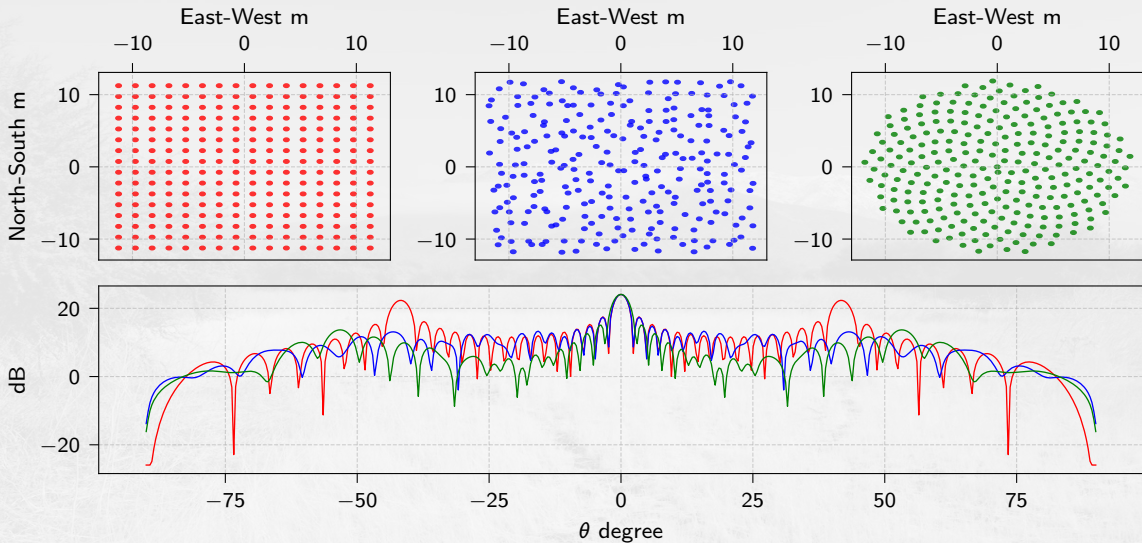
- ANID BASAL FB210003
- ANID / Fondo 2023 QUIMAL/ QUIMAL230001
- Dunlap Seed Fund
- MITACS Globalink



References I

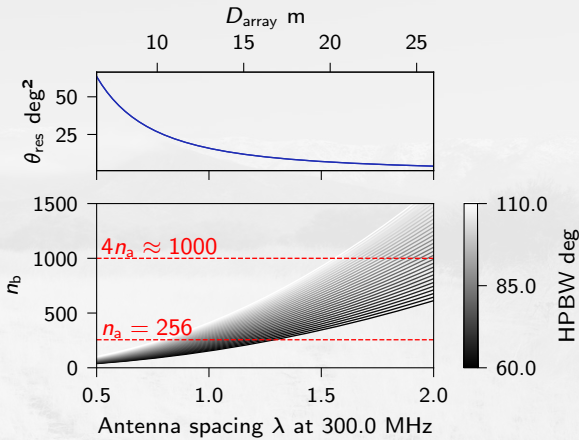
- BeyondPlanck Collaboration, Andersen, K. J., Aurlien, R., et al. 2023, A&A, 675, A1, doi: [10.1051/0004-6361/202244953](https://doi.org/10.1051/0004-6361/202244953)
- Casanelli, T., Leung, C., Rahman, M., et al. 2022, AJ, 163, 65, doi: [10.3847/1538-3881/ac3d2f](https://doi.org/10.3847/1538-3881/ac3d2f)
- Casanelli, T., Mena-Parra, J., Manosalva, S., et al. 2025, in 2025 19th European Conference on Antennas and Propagation (EuCAP), 1–5, doi: [10.23919/EuCAP63536.2025.10999353](https://doi.org/10.23919/EuCAP63536.2025.10999353)
- Chawla, P., Kaspi, V. M., Josephy, A., et al. 2017, ApJ, 844, 140, doi: [10.3847/1538-4357/aa7d57](https://doi.org/10.3847/1538-4357/aa7d57)
- CHIME/FRB Collaboration, Andersen, B. C., Bandura, K. M., et al. 2020, Nature, 587, 54, doi: [10.1038/s41586-020-2863-y](https://doi.org/10.1038/s41586-020-2863-y)
- CHIME/FRB Collaboration, Amiri, M., Andersen, B. C., et al. 2021, ApJS, 257, 59, doi: [10.3847/1538-4365/ac33ab](https://doi.org/10.3847/1538-4365/ac33ab)
- Hickish, J., Abdurashidova, Z., Ali, Z., et al. 2016, Journal of Astronomical Instrumentation, 5, 1641001, doi: [10.1142/S2251171716410014](https://doi.org/10.1142/S2251171716410014)
- Lin, H.-H., Scholz, P., Ng, C., et al. 2024, ApJ, 975, 75, doi: [10.3847/1538-4357/ad779d](https://doi.org/10.3847/1538-4357/ad779d)
- Ling, D. F.-J., Hashimoto, T., Yamasaki, S., et al. 2023, MNRAS, 518, 1398, doi: [10.1093/mnras/stac3018](https://doi.org/10.1093/mnras/stac3018)
- Olausen, S. A., & Kaspi, V. M. 2014, ApJS, 212, 6, doi: [10.1088/0067-0049/212/1/6](https://doi.org/10.1088/0067-0049/212/1/6)
- Swainston, N. A., Lee, C. P., McSweeney, S. J., & Bhat, N. D. R. 2022, PASA, 39, e056, doi: [10.1017/pasa.2022.52](https://doi.org/10.1017/pasa.2022.52)

Array configuration ($d = 1.5\lambda$, $\theta_{\text{res}} = 2.3^\circ$, $n_b = 1226$)



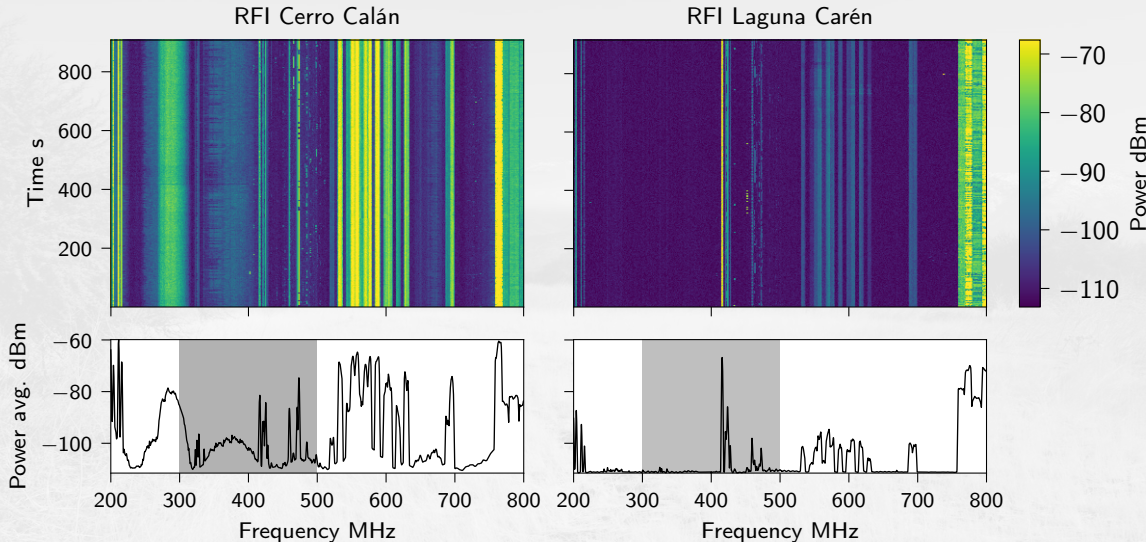
CHARTS field-of-view Ω , beams n_b , and angular resolution θ_{res}

- Angular resolution vs. computation resources
- Complexity $\propto n_a \times n_b$
- CHARTS will cover the full Galactic center $\sim 5 \text{ h d}^{-1}$
- $\Omega \approx 8 \times 10^3 \text{ deg}^2 \rightarrow n_b = 10^3$ (honeycomb lattice)
- Triggered baseband capabilities
 $\theta_{\text{res}} \approx \text{SNR}^{-1}$

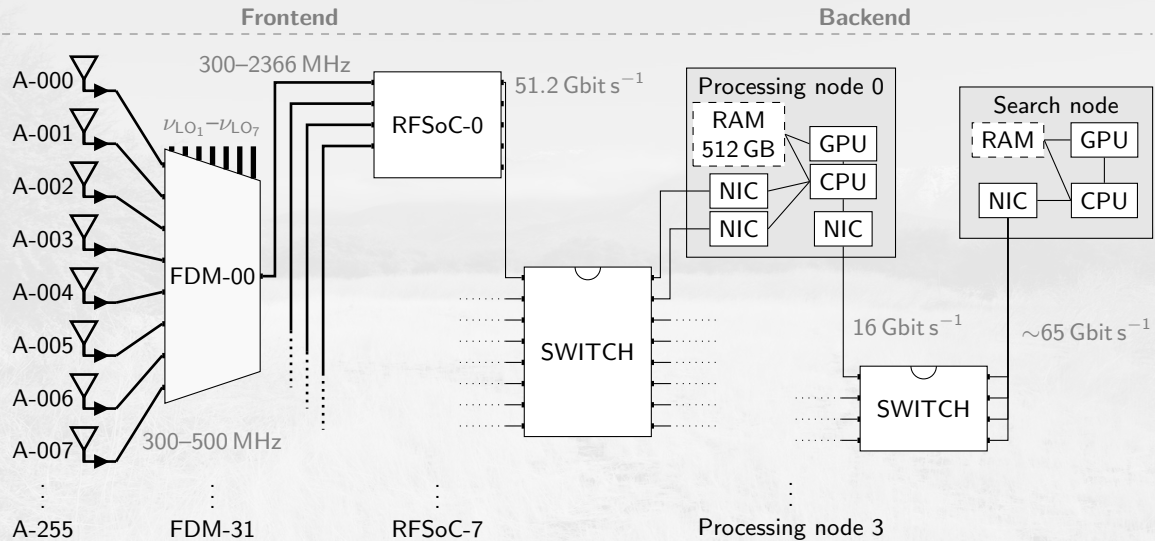


Figure

Radio frequency interference



CHARTS overview



Pulsars frequency spectra J0837+0610

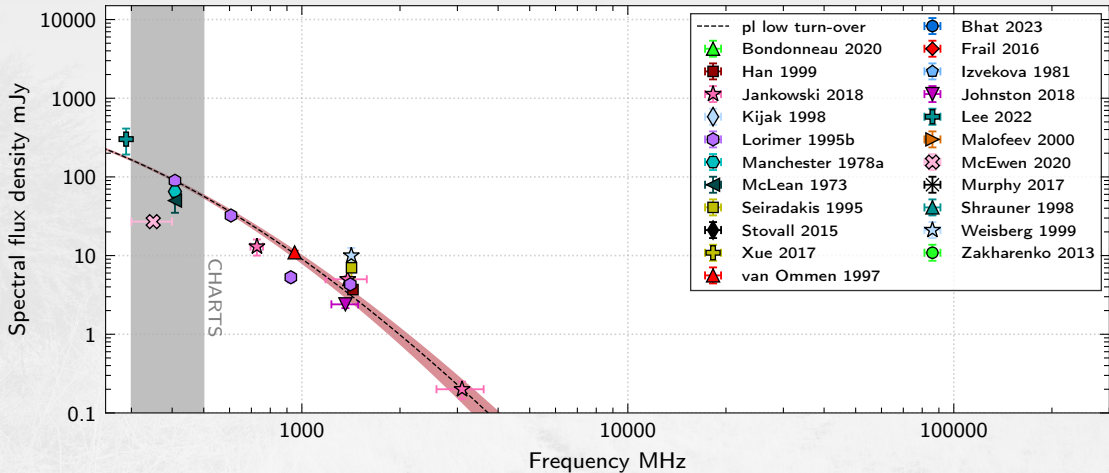


Figure: Frequency spectra for pulsar J0837+0610 (Swainson et al. 2022). Maximum S_ν near 100 MHz, though there are many reason why **not** to observe at those frequencies.

Pulsars frequency spectra Vela

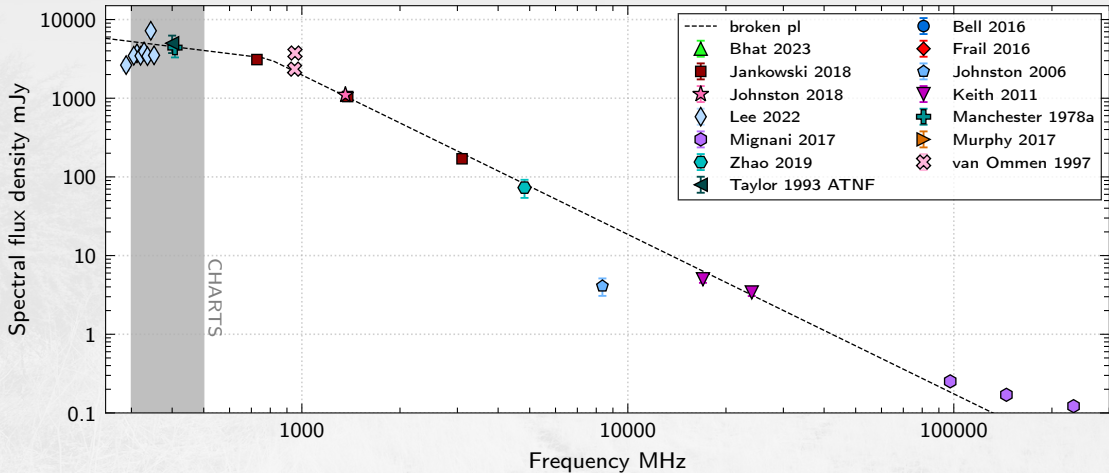


Figure: Frequency spectra for pulsar J0835-4510 (Vela) (Swainson et al. 2022). Maximum S_ν near 100 MHz, though there are many reason why **not** to observe at those frequencies.

Pulsars frequency spectra J2018+2839

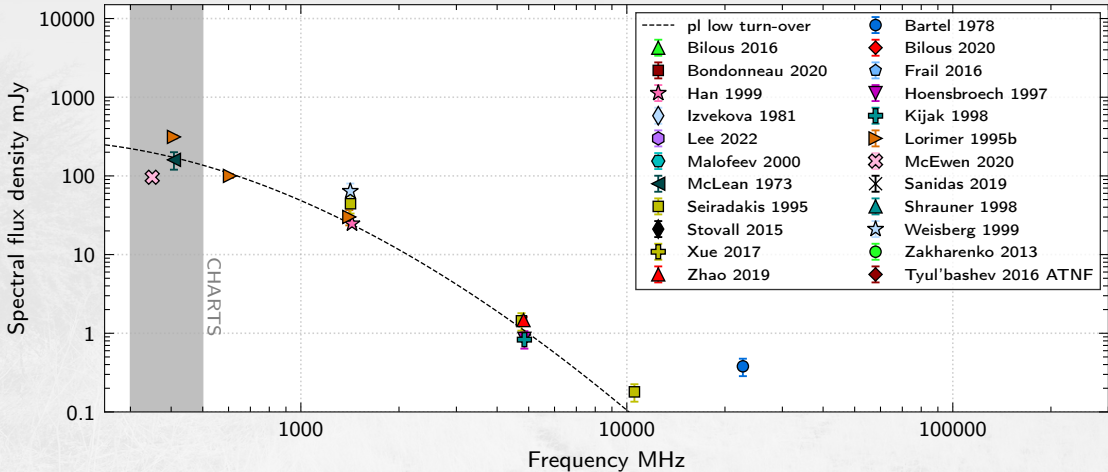


Figure: Frequency spectra for pulsar J2018+2839 (Swainston et al. 2022). Maximum S_ν near 100 MHz, though there are many reason why **not** to observe at those frequencies.

Radio radiation foreground (or frequency spectrum) → an optimum?

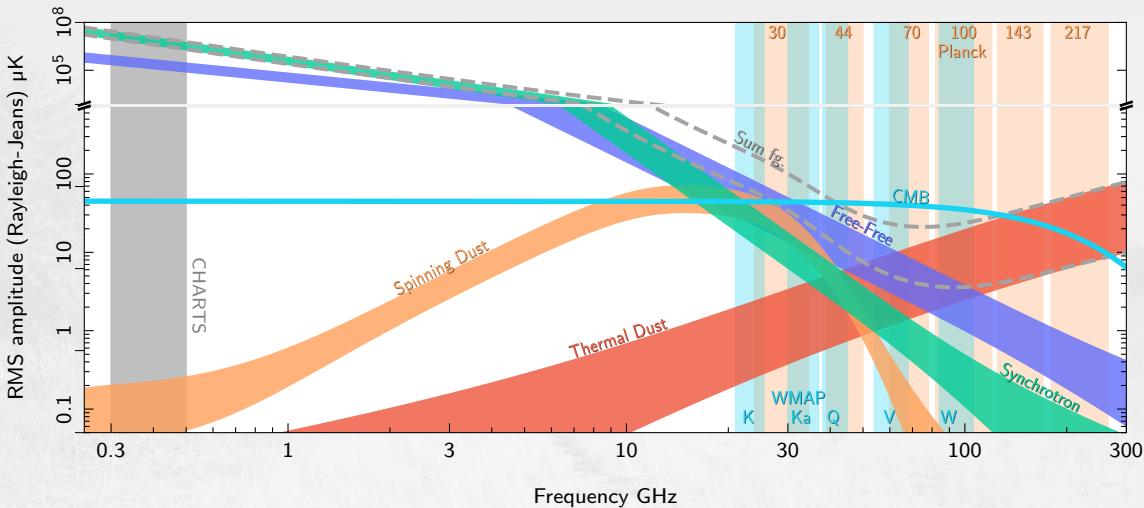
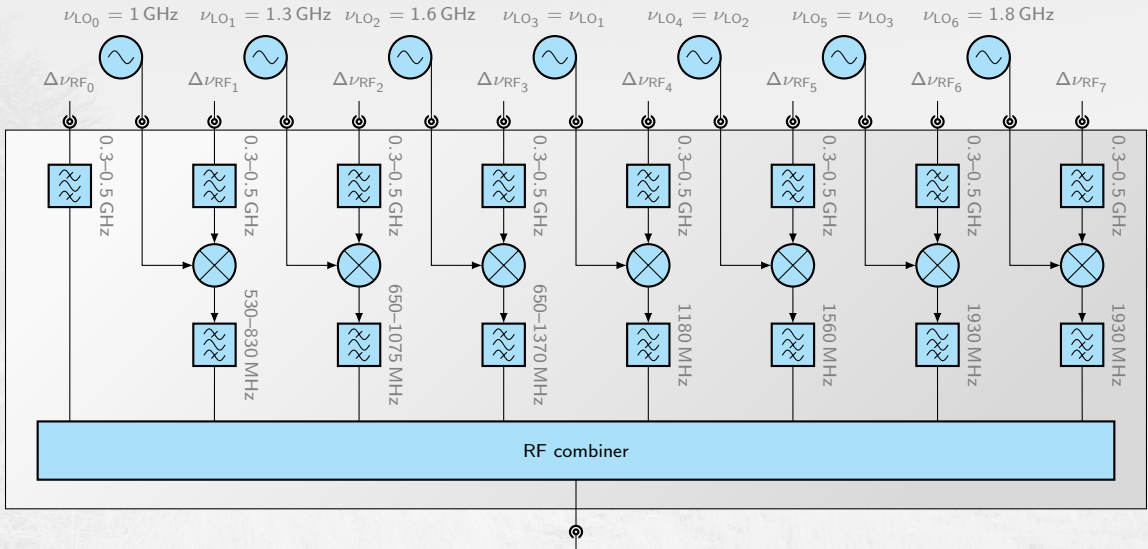


Figure: Adapted from BeyondPlanck Collaboration et al. (2023).

Frequency division multiplexer (FDM)



CHARTS' scientific objectives

① Emission mechanisms

- Magnetospheric emission
- Coherent curvature radiation

② FRB progenitors

- Spiral and dwarf galaxies, globular clusters, etc.

③ Magnetar bursts and bright pulsar giant pulses

- Galactic bright radio bursts
- Super giant pulses

④ New repeating FRBs

- There are only 4 repeating FRBs below $\delta < 0^\circ$
- Optimized for nearby and bright FRBs (low-DM)
- FRBs slightly brighter near 400 MHz

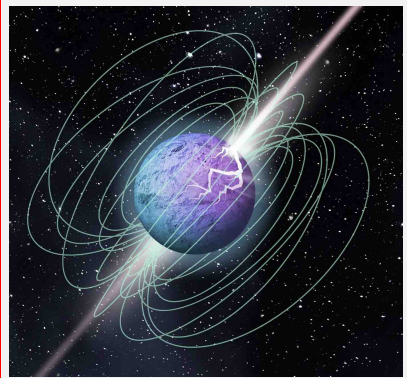


Figure: An artist's impression shows an outburst from a magnetar (McGill University Illustration).

Antenna developments: scaled model

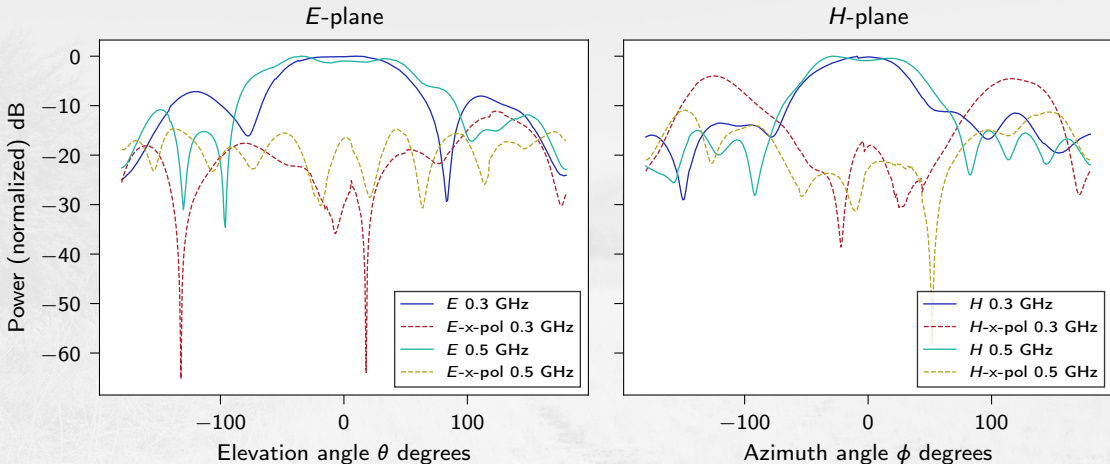


Figure: Antenna power pattern measurements using a 1:5.5 scaled model.

Antenna developments: scaled model

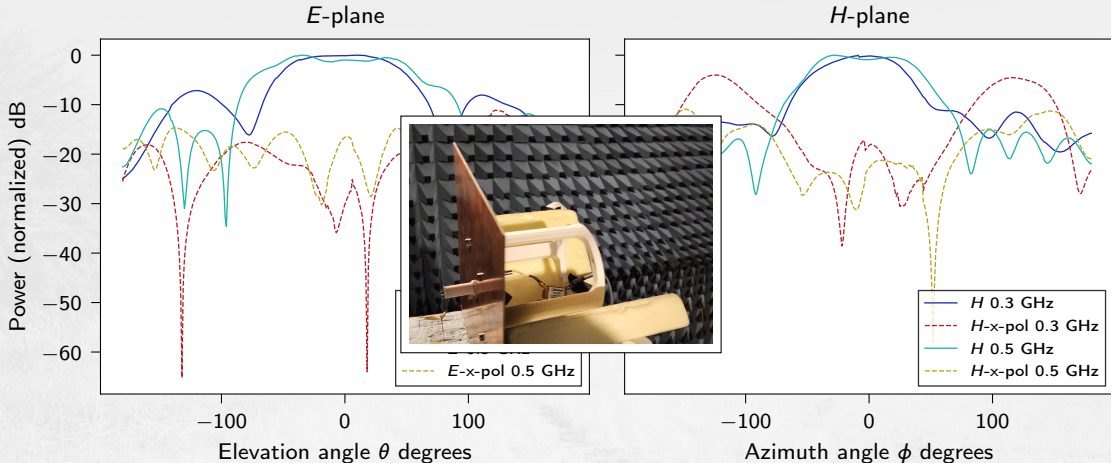


Figure: Antenna power pattern measurements using a 1:5.5 scaled model.

Summary

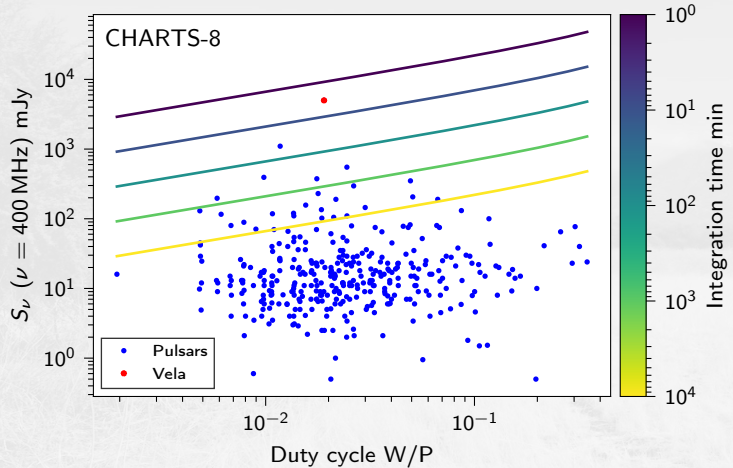


Figure: Pulsar detection CHARTS-8 Southern Hemisphere.

CHARTS team: astronomers, engineers, and physicists

Canada University of Toronto

- Prof. S. Hum (EE)
- Dr. A.W.K. Lau
- Prof. J. Mena-Parra (A&A)
- A. Renard
- Prof. K. Vanderlinde (A&A)

USA Harvard University

- Prof. L. Connor (A&A)

Chile Universidad de Chile

- EE. student O. Arias
- MSc. G. Burgos
- Prof. T. Cassanelli (EE)
- Prof. R. Finger (A&A)
- EE. MSc. student S. Manosalva
- EE. student F. Muñoz
- EE. student B. Pollarolo

